Helicon Plasma Discharge in a Toroidal Magnetic Field of the Tokamak

C. G. Jin, T. Yu, Y. Zhao, Y. Bo, C. Ye, J. S. Hu, L. J. Zhuge, S. B. Ge, X. M. Wu, H. T. Ji, and J. G. Li

***Abstract*—A helicon wave plasma (HWP) discharge in an experimental advanced superconducting tokamak device with a toroidal magnetic field of 2 T is investigated. The HWP with an electron density of 10^{12} cm^{-3} was produced with two 4-turn flat spiral antennas in series that are perpendicular to the toroidal magnetic field and driven by a 13.56-MHz radio-frequency (RF) source at a power of 1500 W, a toroidal magnetic field of 2 T, and a pressure (helium) of 1 Pa. The increase of the toroidal magnetic field from 0.5 to 2 T, the increase of the RF power from 500 to 1500 W, and the decrease of the pressure (helium) from 1 to 0.01 Pa were found to improve the plasma uniformity from the CCD images.**

***Index Terms*—Experimental advanced superconducting tokamak (EAST), helicon, strong magnetic field.**

I. Introduction

FUSION POWER is a promising long-term candidate to supply the energy needs of humanity [1]. The major increase in discharge duration and plasma energy in the next-step fusion reactor such as the International Thermonuclear Experimental Reactor (ITER) will give rise to important plasma–material effects that will critically influence its operation, safety, and performance. The national project of experimental advanced superconducting tokamak (EAST) is the important part of the fusion development stratagem of China, which demands ultravacuum and low impurity level for the plasma discharge. Operation with full metallic wall and molybdenum (Mo) limiters on EAST is also interesting as an ITER-relevant wall material [2], [3]. The plasma-facing components (PFCs) of fusion devices are exposed to extreme environment. Due to intensive particle and heat loads, the surfaces of PFC materials are subjected to material erosion, migration, and redeposition [4]. It has long been recognized that impurities and wall recycling play a critical role in tokamaks. Impurities mainly cause the radiation loss of power and the dilution of hydrogenic species, furthermore impacting plasma stability and global energy confinement [5].

A wide variety of wall-conditioning techniques have been developed and applied in tokamaks for impurity and hydrogen removal [6], [7], such as glow discharge cleaning (GDC) [8], as well as various other methods based on radio-frequency (RF) techniques at electron cyclotron resonance (ECR) [9] and ion cyclotron resonance (ICR) [10]. However, GDC could not work under strong magnetic field. ECR plasmas are poloidally inhomogeneous. Too high vertical field will make ICR plasmas concentrated on the high magnetic field side, which indicated that ICR plasmas are nonuniform. Because high-density plasmas can be achieved by helicon wave plasma (HWP) [11]–[20] discharge in the presence of magnetic fields, HWP discharge plasma is expected to become one of the most effective cleaning ways for impurity removal. Helicon experiments operate over a wide range of parameters, including a variety of power levels, magnetic field strengths, neutral pressures, and magnetic field geometries. Plasma production is much more efficient than with other RF source. Power is coupled through an electromagnetic wave that directly heats the core plasma. High-performance helicon operation with light ions, including hydrogen, deuterium, and helium, with electron density $> 10^{19}$ m^{-3} and gas utilization efficiency η_g ($=$ ions out/atoms in) approaching 100% has been achieved [21], making it worthwhile to develop this type of plasma source for use in EAST wall cleaning. According to a dispersion relationship of the helicon wave, the electron density is proportional to $\mathbf{B_0}$ if the parallel wavenumber is fixed. A strong field is expected to contribute to the better plasma confinement across the field, which would lead to a more efficient plasma production. However, helicon discharges at magnetic field above several kilogauss have not been realized so far [22]. The helicon plasma performance at high magnetic field is still unclear.

In this paper, we present the experimental results of an HWP steady-state discharge in the magnetic field range of 0.5–2 T. Influences of RF power, working pressure, and magnetic field on the HWP discharges are investigated.

II. Experimental Setup

The EAST device (major radius of $R = 1.75$ m and minor radius of $a = 0.4$ m) is the first tokamak in the world with a full

Manuscript received January 29, 2011; revised May 12, 2011; accepted June 22, 2011. Date of publication August 15, 2011; date of current version November 9, 2011. This work was supported in part by the National Magnetic Confinement Fusion Science Program under Grants 2010GB106000 and 2010GB106009, by the National Natural Science Foundation of China under Grants 10975106, 10975105, and 11075114, by the Qing Lan Project, and by a project funded by the Priority Academic Program Development of Jiangsu Higher Education Institutions.

C. G. Jin, T. Yu, Y. Zhao, Y. Bo, C. Ye, S. B. Ge, and X. M. Wu are with the Department of Physics, Soochow University, Soochow 215006, China, and also with the Key Laboratory of Thin Films of Jiangsu, Soochow University, Soochow 215006, China (e-mail: nestajcg@126.com; cye@suda.edu.cn; sbge@suda.edu.cn; xmwu@suda.edu.cn).

J. S. Hu and J. G. Li are with the Institute of Plasma Physics, Chinese Academy of Sciences (ASIPP), Hefei 230031, China (e-mail: hujs@ipp.ac.cn).

L. J. Zhuge is with the Key Laboratory of Thin Films of Jiangsu, Soochow University, Soochow 215006, China, and also with the Analysis and Testing Center, Soochow University, Soochow 215006, China (e-mail: ljzhuge@suda.edu.cn).

H. T. Ji is with the Princeton Plasma Physics Laboratory, Princeton University, Princeton, NJ 08543-0451 USA (e-mail: hji@pppl.gov).

Color versions of one or more of the figures in this paper are available online at http://ieeexplore.ieee.org.

Digital Object Identifier 10.1109/TPS.2011.2161344

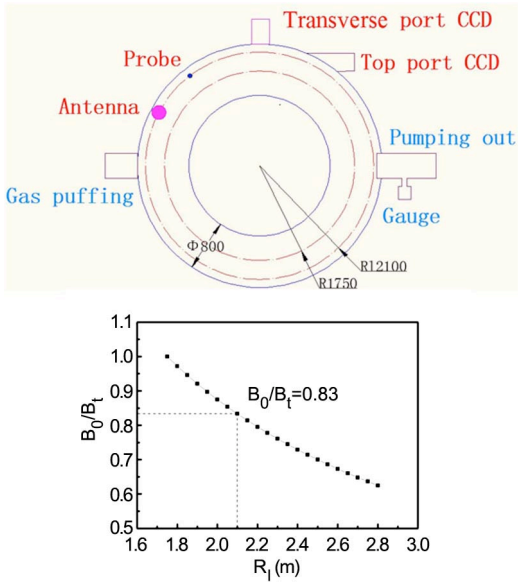

Fig. 1. Schematic spatial arrangement of the antenna on the EAST, relationship between $\mathbf{B_0}$ and $\mathbf{B_t}$.

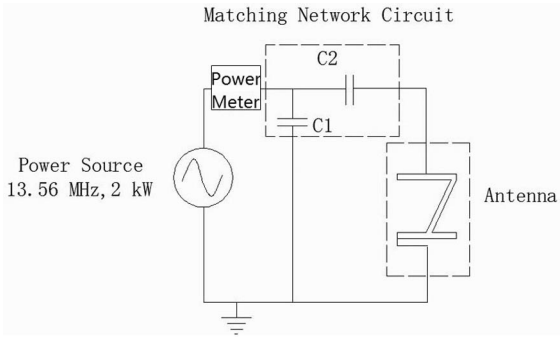

Fig. 2. Schematic of the electric system.

superconducting advanced divertor configuration [3]. Because the steady-state toroidal magnetic field must be maintained at 2 T, the HWP discharges have been carried out at this high magnetic field. Two 4-turn stainless flat spiral antennas in diameter of 13.5 cm were connected in series with a distance of 15 cm. The antennas were placed in the tokamak device at the position of $R_l = 2.1$ m, as shown in Fig. 1. The proportion of the actual magnetic field around the antenna and the set of the values is $R/R_l \approx 0.83$, as shown in Fig. 1. This antenna can excite the azimuthal mode number of $m = 0$ and yields a higher density plasma than a single flat spiral antenna. The 13.56-MHz RF power (PSG-IIIA, Rishige Company Ltd.) was applied to the antennas through a standard L-type capacitive matching network, as shown in Fig. 2. The incident and reflected powers were monitored with in-line power meters between the RF amplifier and tuning circuit with a measurement accuracy of 2%. The reflected power was minimized by adjusting the capacitors (C1 and C2 shown in Fig. 2) in the matching circuit. In the experiment, the toroidal magnetic field from 0.5 to 2 T, the RF power from 500 to 1500 W, and the working pressure from 0.01 to 1 Pa were varied to investigate the influences of RF power, working pressure, and magnetic field on the HWP performance. Helium gas was used as the discharge gas. Four turbopump stations with a nominal pump speed of 12 m^3/s were used for particle exhaust. Calibrated PKR251 Penning gauges were used to monitor the total pressure in the EAST vacuum vessel. A Langmuir probe and a visible CCD camera were used to measure the ion saturation current and the plasma light emission, respectively.

The camera was focused at either the axial or radial center of the chamber depending on its viewing direction, as shown in Fig. 1. As will be discussed in Section III, the light intensity is proportional to $n_e\langle\sigma\nu\rangle$, where n_e is the electron density and $\langle\sigma\nu\rangle$ is a steep function of electron temperature T_e. The 2-D patterns seen with the CCD camera were therefore caused by a convolution of T_e and n_e variations, but these could not be separated because a 2-D Langmuir probe drive was not available.

III. Results and Discussion

Fig. 3 shows the photographs of helicon discharge plasmas at the toroidal magnetic fields of 0.5, 1, and 2 T, respectively, which were taken from the top port in the neighborhood of the antenna. The HWPs were observed by the CCD camera at the top port; it shows that they seemed toroidally symmetric and concentrated on the center of the antenna in the radial direction which indicated that the HWPs were toroidally uniform (like on circular machines). However, all the photographs present poloidal asymmetric emission and alternately dark and bright striations in the plasma region. This may be attributed to the asymmetric poloidal magnetic field and the antenna configuration. In order to investigate the HWP discharge parameters, a Langmuir probe [23] was used to measure the plasma density at $\mathbf{B_t} = 2$ T, $p_{\mathrm{He}} = 1$ Pa, and $P_{\mathrm{inp}} = 1500$ W. This result shows that the high electron density near 10^{12} cm^{-3} was successfully achieved, which belongs to the typical HWP density range. Again, we assumed that the emission is the result of single collisions between electrons and atoms in the ground state, followed by direct radiating de-excitation. Although absolute numbers of the emitting level of the excited atoms or ions may sometimes be desirable, it is often more important to obtain information about the overall ion density or the electron temperature in the plasma. In order to link the excited level population to any of these quantities, a model must be used. A good discussion about the models that can be used to describe the different types of plasmas can be found in [24]. For plasma conditions observed in a helicon source, the simple steady-state corona model can be used within a common range (10^{11} $\mathrm{cm}^{-3} < n_e < 10^{12}$ cm^{-3} for helium) to predict the population of the excited levels. In order to use this model, the plasma must satisfy the following conditions [24]: The electron velocity distribution can be described by a Maxwellian distribution, the ion and neutral temperatures are less than the electron temperature, and the plasma is optically thin to its own radiation [25]. A balance between the rate of collisional excitation from the ground level and the rate of spontaneous radiative decay determines the population densities of the excited levels. Let us assume that each line emission is the result of single collisions between

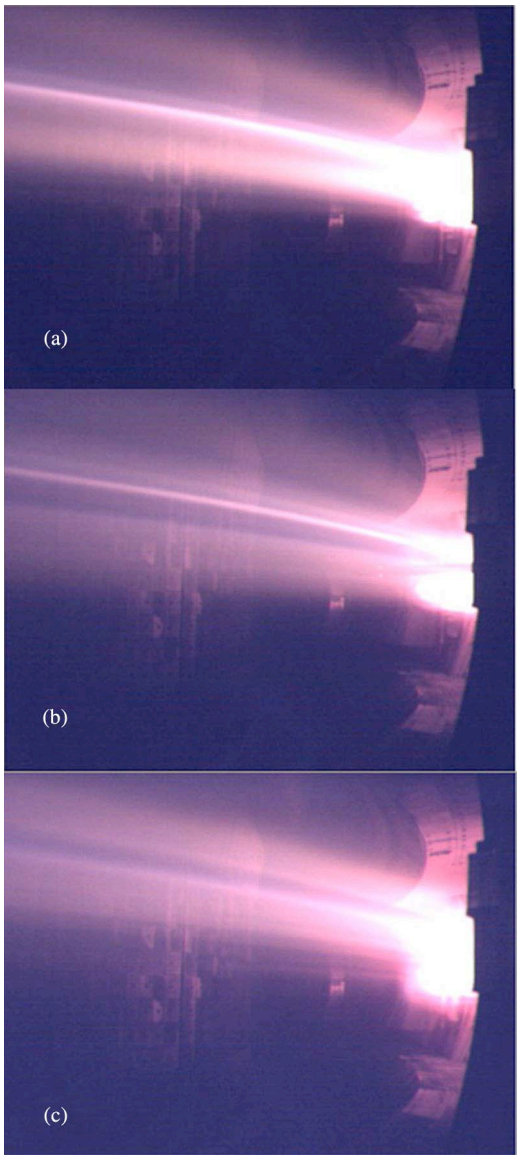

Fig. 3. Photographs taken from the top port in the neighborhood of the antenna, changing the toroidal magnetic field, with a pressure of $p_{\mathrm{He}} = 1$ Pa and an RF power of $P_{\mathrm{inp}} = 1500$ W. (a) 0.5 T. (b) 1 T. (c) 2 T.

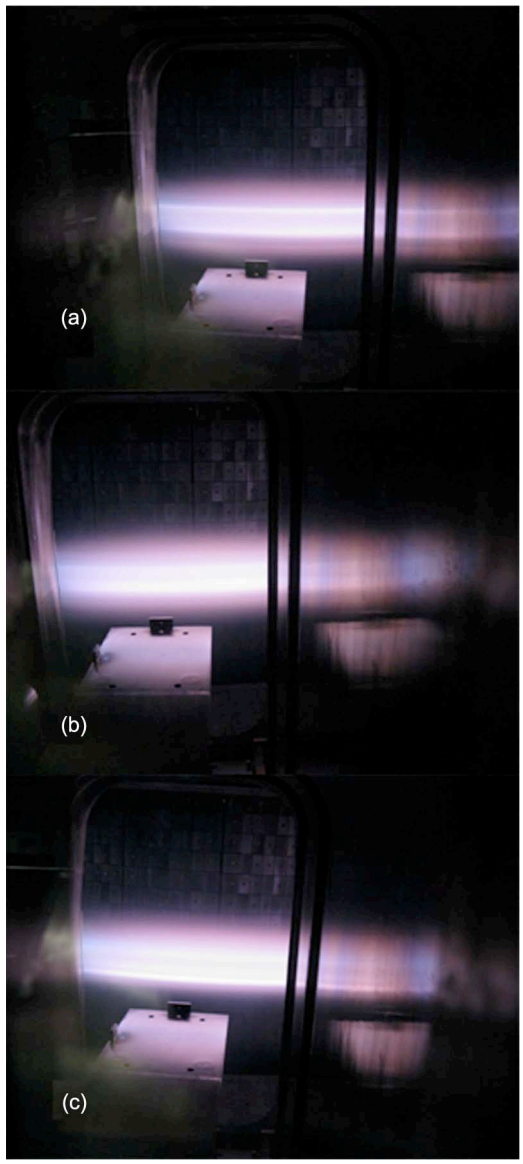

Fig. 4. Transverse images of the discharge, changing the toroidal magnetic field, with a pressure of $p_{\mathrm{He}} = 1$ Pa and an RF power of $P_{\mathrm{inp}} = 1500$ W. (a) 0.5 T. (b) 1 T. (c) 2 T.

electrons and atoms in the ground state. The population of level j (N_j) is given by [24]

$$n_e N_0 \langle \sigma\nu \rangle_{0j} = N_j \sum_{i<j} A_{ji} \tag{1}$$

where N_0 is the population of the ground level, $\sum_{i<j} A_{ji}$ is the total transition probability from level j to all lower states, and $\langle \sigma\nu \rangle_{0j}$ is the excitation rate coefficient for the electron impact excitation of level j from ground state. Thus, from the emitter population, provided that one knows the excitation rate coefficient for this level and the different transition probabilities associated with this level, one can evaluate the ion density. With the magnetic field increase, the broadening of the light emission column is observed; meanwhile, the uniformity of the emission becomes better. This may reflect the increased radial confinement of ions with the increase of $\mathbf{B_t}$, for low $\mathbf{B_t}$ radiation losses deplete the plasma, giving rise to an axial density gradient and a consequently lower density at the plasma edge observed from Fig. 3. The higher the magnetic field which helps to confine the electrons for longer time and transport the inductive field into the entire plasma, the more ionization rate can be achieved. To verify the emission profile, the transverse images of the plasma at the axial positions with the different magnetic fields are shown in Fig. 4. The result in Fig. 4 shows that the plasma column becomes broader and more uniform with the increase in the magnetic field, which is consistent with Fig. 3.

Fig. 5 shows the photographs of the helicon discharge plasma at the input RF powers of 500, 1000, and 1500 W, respectively, with a pressure of $p_{\mathrm{He}} = 1$ Pa and a magnetic field of $\mathbf{B_t} = 2$ T, which were also taken from the top port in the neighborhood of the antenna. It can be seen that the plasma transforms into a mode with a bright density central core with increased RF

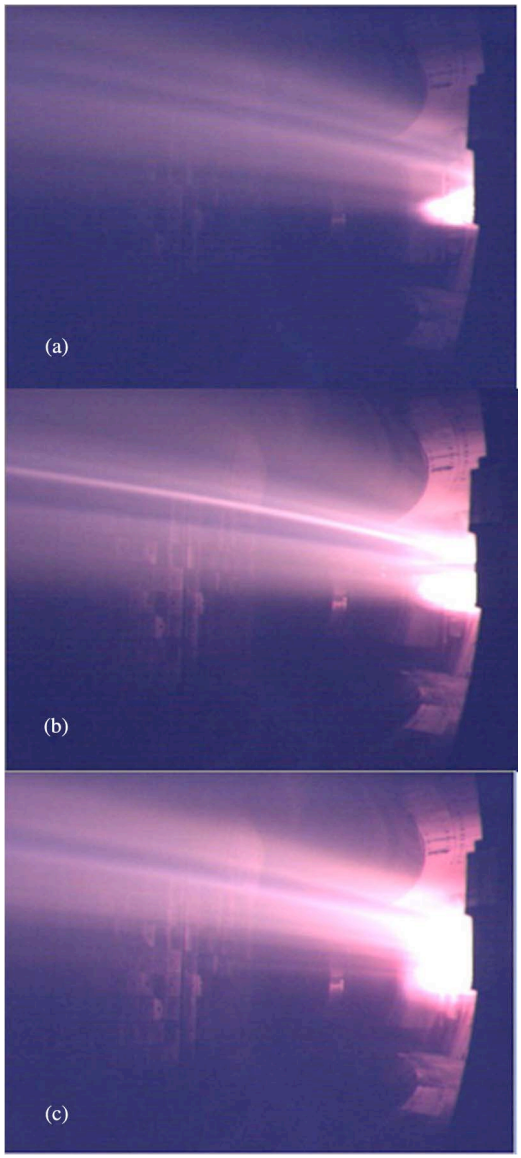

Fig. 5. Photographs taken from the top port in the neighborhood of the antenna, changing the input RF power $P_{\rm inp}$, with a pressure of $p_{\rm He} = 1$ Pa and a magnetic field of $\mathbf{B_t} = 2$ T. (a) 500 W. (b) 1000 W. (c) 1500 W.

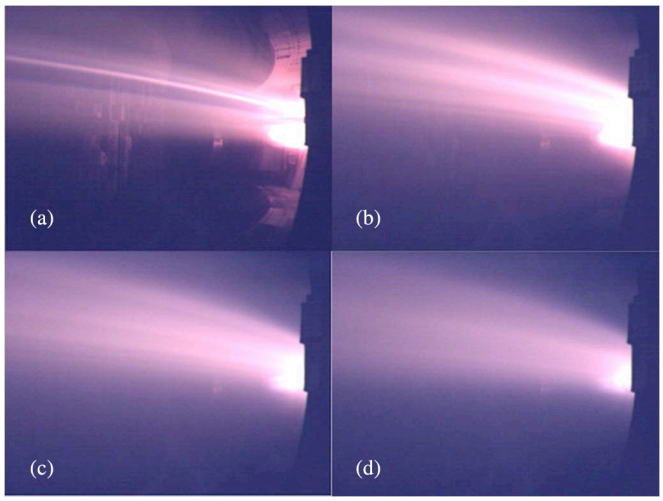

Fig. 6. Photographs taken from the top port in the neighborhood of the antenna, changing the pressure, with an RF power of $P_{\rm inp} = 1000$ W and a magnetic field of $\mathbf{B_t} = 2$ T. (a) 1 Pa. (b) 0.1 Pa. (c) 0.05 Pa. (d) 0.01 Pa.

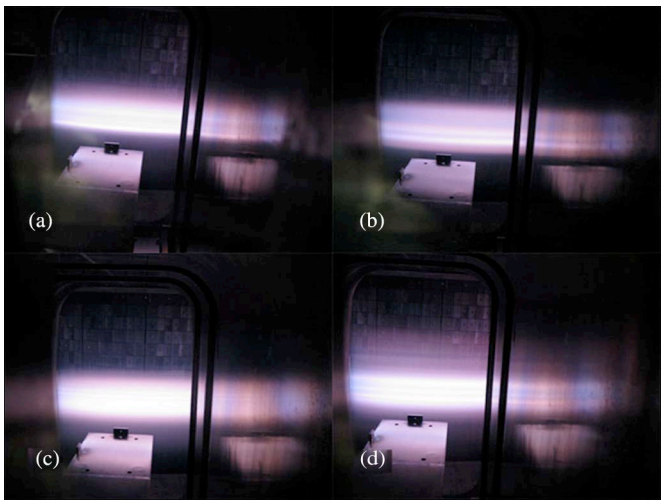

Fig. 7. Transverse images of the discharge, changing the pressure, with an RF power of $P_{\rm inp} = 1000$ W and a magnetic field of $\mathbf{B_t} = 2$ T. (a) 1 Pa. (b) 0.1 Pa. (c) 0.05 Pa. (d) 0.01 Pa.

power. This core has higher T_e and higher ionization fraction than the diffused plasma. Furthermore, it is interesting to note that higher densities are possible with increased power levels while high ionization efficiencies are possibly maintained. Higher RF power may produce HWP with higher electron density. This may be attributed to the increase of the RF power which gives rise to the increase in electron density, which gains energy by TG mode. A greater input power may be necessary to facilitate higher plasma density.

Fig. 6 shows the pictures of the plasma at $\mathbf{B_t} = 2$ T and $P_{\rm inp} = 1000$ W, with different work pressures, which were also taken from the top port in the neighborhood of the antenna. It is easily found that, as the work pressure decreases, the intensity of emission reduces, and the column of emission becomes more uniform. To make exactly certain the changes in plasma parameters, the transverse images of the discharge with different work pressures are shown in Fig. 7. The result in Fig. 7 shows that the plasma column becomes more uniform and the intensity of emission becomes weak with decreasing work pressure, which is consistent with Fig. 6. According to the Clapeyron equation $(pV = N_0RT)$ and (1), N_0 decreases with work pressure (p) decreasing. Therefore, emission intensity decreases with decreasing work pressure. Meanwhile, the density increases as the pressure is decreased because the total collision frequency decreases when more helium gas is exhausted out the discharge chamber. Meanwhile, at low pressures, the mean free path for ionization is longer than the chamber, and the majority of the energetic electrons are lost axially to the walls without ionizing. The electrons are heated when more gas is exhausted out the chamber and will tend to diffuse toward regions of low density with less collision, which may induce better uniformity of the plasma [11]. However, the coupling mechanism of the $m = 0$ mode is not yet understood, and its origin is still under dispute.

IV. Summary

An HWP discharge in the EAST device with a toroidal magnetic field of 2 T has been first investigated. Helium plasma density near 10^{12} cm^{-3} had been measured by a Langmuir probe at the conditions of a magnetic intensity of 2 T, a working gas pressure of 1 Pa, and an RF power of 1500 W with a frequency of 13.56 MHz. In the experiments, some experimental phenomena were found from the CCD images. The results show that the uniformity of the plasma was improved with the increase of the toroidal magnetic field from 0.5 to 2 T, the increase of the RF power from 500 to 1500 W, and the decrease of the pressure from 1 to 0.01 Pa.

References

[1] R. Toschi, "Nuclear fusion, an energy source," *Fusion Eng. Des.*, vol. 36, no. 1, pp. 1–8, Apr. 1997.

[2] Y. X. Wan, L. Jiangang, and W. Peide, "First engineering commissioning of EAST Tokamak," *Plasma Sci. Technol.*, vol. 8, no. 3, pp. 253–254, May 2006.

[3] X. Gao, J. Li, B. Wan, J. Zhao, L. Hu, H. Liu, Y. Jie, Q. Xu, Z. Wu, Y. Yang, X. Gong, B. Shen, J. Hu, Y. Shi, B. Ling, J. Wang, S. Sajjad, Q. Zang, W. Gao, T. Zhang, Y. Yu, Y. Yang, X. Han, N. Shi, T. Ming, A. Ti, W. Zhang, G. Xu, J. Chen, G. Luo, X. Zhang, J. Mao, and Y. Wan, "Extension of operational limits on EAST," *Nucl. Fusion*, vol. 47, no. 9, pp. 1353–1357, Oct. 2007.

[4] A. Litnovsky, V. Philipps, A. Kirschner, P. Wienhold, G. Sergienko, A. Kreter, U. Samm, O. Schmitz, K. Krieger, P. Karduck, M. Blome, B. Emmoth, M. Rubel, U. Breuer, and A. Scholl, "Transport of carbon, deposition and fuel accumulation in metallic castellated limiters exposed in the SOL of TEXTOR," *J. Nucl. Mater.*, vol. 367–370, pp. 1481–1486, Apr. 2007.

[5] E. de la Cal and E. Gauthier, "First-wall cleaning and isotope control studies by ICRF conditioning in Tore Supra with a permanent magnetic field," *Plasma Phys. Control. Fusion*, vol. 39, no. 7, pp. 1083–1099, Jul. 1997.

[6] J. Li, Y. P. Zhao, X. M. Gu, C. F. Li, B. N. Wan, X. D. Zhang, J. R. Luo, X. Z. Gong, J. K. Xie, Y. X. Wan, P. J. Qin, X. M. Wang, Y. D. Meng, S. F. Li, X. Gao, Y. Yang, D. Y. Xue, Y. Z. Mao, X. Den, L. Chen, Y. C. Fang, F. X. Yin, S. X. Liu, X. K. Yang, D. Z. Xu, J. Y. Ding, Y. X. Jie, Q. C. Zhao, J. S. Mao, S. Y. Zhang, J. Y. Zhao, J. S. Hu, H. Y. Fan, M. S. Wei, B. L. Lin, G. X. Wang, Y. D. Fang, and W. C. Shen, "ICRF boronization—A new technique towards high efficiency wall coating for superconducting tokamak reactors," *Nucl. Fusion*, vol. 39, no. 8, pp. 973–978, Aug. 1999.

[7] G. Federici, C. H. Skinner, J. N. Brooks, J. P. Coad, C. Grisolia, A. A. Haasz, A. Hassanein, V. Philipps, C. S. Pitcher, J. Roth, W. R. Wampler, and D. G. Whyte, "Plasma–material interactions in current tokamaks and their implications for next step fusion reactors," *Nucl. Fusion*, vol. 41, no. 12, pp. 1967–2137, Dec. 2001.

[8] W. Poschenrieder, G. Staudenmaier, and P. Staib, "Conditioning of ASDEX by glow discharge," *J. Nucl. Mater.*, vol. 93–94, pp. 322–329, Oct. 1980.

[9] A. Sagara, M. Iima, S. Inagaki, N. Inoue, H. Suzuki, K. Tsuzuki, S. Masuzaki, J. Miyazawa, and O. Motojima, "Wall conditioning at the starting phase of LHD," *J. Plasma Fus. Res.*, vol. 75, no. 3, pp. 263–267, Mar. 1999.

[10] E. Gauthier, E. de la Cal, B. Beaumont, A. Becoulet, C. Gil, C. Grisolia, A. Grosman, T. Hutter, H. Kuus, L. Ladurelle, and J. L. Segui, "Wall conditioning technique development in Tore Supra with permanent magnetic field by ICRF wave injection," *J. Nucl. Mater.*, vol. 241–243, pp. 553–538, Feb. 1997.

[11] M. A. Lieberman and A. J. Lichtenberg, *Principles of Plasma Discharges and Materials Processing*. New York: Wiley, 1994.

[12] S. Shinohara, "Propagating wave characteristics for plasma production in plasma processing field," *Jpn. J. Appl. Phys.*, vol. 36, no. 7B, pp. 4695–4703, Apr. 1997.

[13] R. W. Boswell and F. F. Chen, "Helicons—The early years," *IEEE Trans. Plasma Sci.*, vol. 25, no. 6, pp. 1229–1244, Dec. 1997.

[14] F. F. Chen and R. W. Boswell, "Helicons—The past decade," *IEEE Trans. Plasma Sci.*, vol. 25, no. 6, pp. 1245–1257, Dec. 1997.

[15] S. Shinohara, "Recent topics on high density plasma production by helicon waves," *J. Plasma Fusion Res.*, vol. 78, no. 1, pp. 5–18, Jan. 2002.

[16] I. G. Brown, *The Physics and Technology of Ion Sources*, 2nd ed. Weinheim, Germany: Wiley, 2004.

[17] A. Goncharov, A. Dobrovolsky, A. Zatuagan, and I. Protsenko, "High-current plasma lens," *IEEE Trans. Plasma Sci.*, vol. 21, no. 5, pp. 573–577, Oct. 1993.

[18] A. Goncharov, I. Protsenko, G. Yushkov, and I. Brown, "Focusing of high-current, large-area, heavy-ion beams with an electrostatic plasma lens," *Appl. Phys. Lett.*, vol. 75, no. 7, pp. 911–913, May 1999.

[19] J. J. Su, T. Katsouleas, and J. M. Dawson, "Plasma lenses for focusing particle beams," *Phys. Rev. A, At. Mol. Opt. Phys.*, vol. 41, no. 6, pp. 3321–3331, Mar. 1990.

[20] R. W. Boswell, "Very efficient plasma generation by whistler waves near the lower hybrid frequency," *Plasma Phys. Control. Fusion*, vol. 26, no. 10, pp. 1147–1162, Oct. 1984.

[21] J. P. Squire, F. R. Chang-Díaz, T. W. Glover, V. T. Jacobson, G. E. McCaskill, D. S. Winter, F. W. Baity, M. D. Carter, and R. H. Goulding, "High power light gas helicon plasma source for VASIMR," *Thin Solid Films*, vol. 506–507, pp. 579–582, May 2006.

[22] S. Shinoharaa and H. Mizokoshi, "Development of a strong field helicon plasma source," *Rev. Sci. Instrum.*, vol. 77, no. 3, pp. 036108–036111, Mar. 2006.

[23] L. Oksuz and N. Hershkowitz, "Understanding Mach probes and Langmuir probes in a drifting, unmagnetized, non-uniform plasma," *Plasma Sources Sci. Technol.*, vol. 13, no. 2, pp. 263–271, May 2004.

[24] R. W. P. McWhirter, *Spectral, Intensities, in Plasma Diagnostic Techniques*. New York: Academic, 1965, ch. 5.

[25] R. F. Boivin, "Mean optical depth and optical escape factor for helium transitions in helicon plasmas," West Virginia Univ., Morgantown, WV, WV-PL-045, 2000.

C. G. Jin, photograph and biography not available at the time of publication.

T. Yu, photograph and biography not available at the time of publication.

Y. Zhao, photograph and biography not available at the time of publication.

Y. Bo, photograph and biography not available at the time of publication.

C. Ye, photograph and biography not available at the time of publication.

J. S. Hu, photograph and biography not available at the time of publication.

L. J. Zhuge, photograph and biography not available at the time of publication.

S. B. Ge, photograph and biography not available at the time of publication.

X. M. Wu, photograph and biography not available at the time of publication.

H. T. Ji, photograph and biography not available at the time of publication.

J. G. Li, photograph and biography not available at the time of publication.